

First-principles prediction of mechanical and bonding characteristics of new T_2 superconductor Ta_5GeB_2

M. A. Hadi^{*1}, M. T. Nasir², M. Roknuzzaman³, M. A. Rayhan², S. H. Naqib¹ and A. K. M. A. Islam^{1,4}

¹ Department of Physics, University of Rajshahi, Rajshahi-6205, Bangladesh

² Department of Arts & Science, Bangladesh Army University of Science & Technology, Saidpur-5310, Nilphamari, Bangladesh

³ Department of Physics, Jessore University of Science and Technology, Jessore-7408, Bangladesh

⁴ International Islamic University Chittagong, 154/A College Road, Chittagong-4203, Bangladesh

Received ZZZ, revised ZZZ, accepted ZZZ

Published online ZZZ(Dates will be provided by the publisher.)

Keywords T_2 superconductor; First-principles method; Mechanical properties; Bonding nature

* Corresponding author: E-mail hadipab@gmail.com, Phone: +88 01716200042

Abstract

In the present paper, DFT (Density Functional Theory) based first-principles methods are applied to investigate the mechanical and bonding properties of newly synthesized T_2 phase superconductor Ta_5GeB_2 for the first time. The calculated lattice constants are in reasonable agreement with the experiment. The elastic constants (C_{ij}), bulk modulus (B), shear modulus (G), Young's modulus (Y), Poisson ratio (ν), Pugh ratio (G/B), and elastic anisotropy factor A of Ta_5GeB_2 are calculated and used to explore the mechanical behavior of the compound. To give an explanation of the bonding nature of this new ternary tetragonal system, the band structure, density of states, and Mulliken atomic population are investigated. The estimated Debye temperature and Vickers hardness are also used to justify both the mechanical and bonding properties of Ta_5GeB_2 .

1 Introduction

Very recently, Corrêa et al. [1] synthesized a new compound Ta_5GeB_2 belonging to the tetragonal T_2 phase with Cr_5B_3 prototype structure that is stabilized by substituting Ge for B at the 8h Wyckoff position. In addition to magnetization, electrical resistivity and heat capacity measurements, they also reported on the bulk superconductivity of this compound with a transition temperature $T_C \sim 3.8$ K. The T_2 phases are labeled as “5-3” metal-metalloid compounds which fall in the large group of metal based systems spanning from the alkaline-earth metal to the late transition metals. These phases comprise more than 40 compounds of the general formula M_5X_3 (M = metal, X = semi-metal or non-metal), which form tetragonal crystal structure, usually known as the Cr_5B_3 type [2]. The T_2 structure also retains a rather high-coordination number of metal–metal atomic bonds to maintain a fairly close-packed structure [3,4]. In addition, the T_2 crystal structure retains a body-centered symmetry similar to refractory metals. The majority of these materials crystallize into the space group $I4/mcm$ (No. 140). Some lower symmetry distorted variants are also known. In accordance with the occupied crystallographic sites in $I4/mcm$, the general composition M_5X_3 can be rewritten as $M(1)M(2)_4X(1)X(2)_2$. There are significant differences in the cell dimensions and site parameters among some compounds, though most of them crystallize in the same space group. In fact, the Cr_5B_3 type is divided into two isopointal subfamilies, namely major and minor subfamilies [5,6]. All the members of the major subfamily known to date are typified by a c/a ratio of about 1.85 and by the formation of $X(2)_2$ dumbbells. The shortest inter-atomic distance in the major subfamily occurs between two $X(2)$ atoms. This distance is due to a covalent single bond. The compound Cr_5B_3 falls in this subfamily. This subfamily is also known as Cr_5B_3 subfamily. The minor subfamily, the so-called In_5Bi_3 subfamily, includes three binary compounds as its members. The members In_5Bi_3 and Tl_5Te_3 [5,7-14] of this subfamily are well known. In these compounds, the c/a ratio is about 1.45 and no dumbbells are seen to occur. Shorter interatomic distances are observed between $M(1)$ and $X(1)$ atoms in a linear chain along $[001]$ in this subfamily.

T_2 phase tenders a collection of fascinating properties, such as high-melting temperature [15], oxidation resistance [16-18], and advantageous high-temperature mechanical properties [19-21]. As the focal point of the microstructure designs with the T_2 ternary phase, the primary basis of the alloying nature in this phase together with the communal solid solution of a wide range of transition metals has been formed in accordance with the governing geometric and electronic aspects. In a multi-phase alloy the materials show evidence of high-temperature creep strength [22,23] and ambient temperature flexural strength [24]. The remarkable properties of the multi-phase alloys have raised the interest in the monolithic T_2 phase. For instance, the recent data from the room temperature Vickers indentation tests point out that the hardness and the fracture toughness for the T_2 phase are about 30% higher than those of the T_1 phase [25]. In addition, the accumulation of congenital vacancies has been exposed to perform an important task in development of dislocation and precipitation reactions in the T_2 phase that have direct impact on high-temperature structural performance. The typically slow diffusion rates inside the T_2 phase have also been quantified and used to the materials processing approaches.

In the present study, a detailed theoretical investigation of the ground state mechanical and bonding properties of new T_2 phase superconductor Ta_5GeB_2 has been done within the plane wave pseudopotential technique. The mechanical behaviors are analyzed in terms of the single crystal elastic constants and polycrystalline elastic moduli. The bonding characteristics are described by means of electronic band structure, electron energy density of states and Mulliken atomic populations.

2 Methods of calculations

The DFT [26,27] calculations are carried out on the new T_2 superconductor Ta_5GeB_2 using the CASTEP (Cambridge Serial Total Energy Package) code [28]. The computations are performed in a unit cell containing four formula units with 32 atoms (20 Ta, 4 Ge, and 8 B). The GGA-PBE exchange-correlation [29] is applied with the plane-wave pseudopotential available in the above mentioned code. The Vanderbilt-type ultrasoft pseudopotential [30] is used to take care of electron-ion interactions. For sampling the first Brillouin zone, a k-point grid of $7 \times 7 \times 4$ mesh according to Monkhorst-Pack scheme [31] is set for all calculations providing a spacing of 0.02 \AA^{-1} . An energy cutoff of 500 eV is chosen in order to limit the number of plane-waves in the expansion. The BFGS (Broyden-Fletcher-Goldfarb-Shanno) minimization method [32] is utilized for searching the ground state of crystal. All calculations are accomplished under zero pressure, allowing all atomic sites, lattice constants and angles to fully relax. To optimize the system geometry, the chosen tolerances are: total energy difference per atom within 5×10^{-6} eV, maximum ionic Hellmann-Feynman force within 0.01 eV/\AA , maximum stress under 0.02 GPa, and maximum ionic displacement under $5 \times 10^{-4} \text{ \AA}$. The elastic constants, band structure, density of states, and Mulliken atomic population of the new compound are extracted from the fully geometry optimized state.

3 Results and Discussions

3.1 Structural properties

The T_2 phase Ta_5GeB_2 has been found to crystallize in the tetragonal structure D_{8h} with space group $I4/mcm$ (No. 140). Here, the atom Ta is at 4c (0, 0, 0) and 16l ($x, x + 1/2, z$) Wyckoff positions. At the same time, the p elements Ge and B are positioned at 4a (0, 0, 1/4) and 8h ($x, x + 1/2, 0$) Wyckoff positions, respectively. Ta_5GeB_2 structure [Fig.1] is formed by alternate layers. The first one is at ($z = 0$) including both the metal Ta and the p element B, the second ($z = 1/8$) only the transition metal, the third ($z = 1/4$) only the p element Ge, the fourth ($z = 3/8$) only metal Ta, the fifth ($z = 1/2$) comprising both the metal Ta and the p element B. The other layers are due to the tetragonal centered symmetry. For transition metal and p element alloys, the D_{8h} structure shows stability when the concentration of the valence electron are from 4.3 to 5.5 [33]. With a valence electron concentration of 4.375, the new T_2 phase Ta_5GeB_2 satisfies the above stability condition. Optimized lattice constants and x parameters of Ta_5GeB_2 are listed in Table 1 along with those obtained for some other isostructural compounds. The computed lattice constants deviate less than 1.8 % of the experimental values. The evaluated lattice constants are slightly larger than the measured values, which is a general trend inherent to GGA calculations.

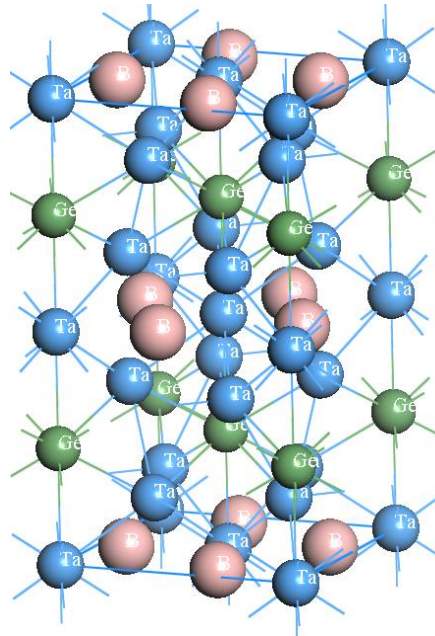


Figure 1 Crystal structure of new T_2 superconductor Ta_5GeB_2 .

Table 1

Structural parameters for Ta₅GeB₂ with the different T₂ phases of D8₁ structure, space group *I4/mcm*, transition metal in 4c and 16l, Si/Ge and B in 4a and 8h.

T ₂ phases	<i>a</i> (Å)	<i>c</i> (Å)	<i>c/a</i>	<i>x</i> _{8h}	<i>x</i> _{16l}	<i>z</i> _{16l}	References
Ta ₅ GeB ₂	6.334	11.785	1.861	0.3827	0.1663	0.1381	Calc. [This]
	6.239	11.578	1.856				Expt. [1]
Nb ₅ SiB ₂	6.245	11.655	1.866	0.6123	0.1695	0.1375	Calc. [34]
Mo ₅ SiB ₂	6.037	11.114	1.841				Calc. [35]
	6.03	11.0	1.824				Calc. [36]
	6.013	11.0485	1.837	0.375	0.1653	0.1388	Expt. [3]
	6.0272	11.0671	1.836	0.3784	0.1641	0.1398	Expt. [37]
	6.001	11.022	1.837				Expt. [38]

3.2 Elastic properties

The elastic constants are computed within the CASTEP module from the first-principles method by using a set of uniform deformations of a finite value. The resulting stresses are then computed by optimizing the internal degrees of freedoms [39]. The Voigt-Reuss-Hill approximations [40-42] are used to calculate the polycrystalline bulk modulus (*B*) and shear modulus (*G*). The equations, $Y = (9GB)/(3B + G)$ and $\nu = (3B - 2G)/(6B + 2G)$ are also used to evaluate the Young's modulus *Y* and Poisson ratio ν , respectively.

The six elastic constants (*C*₁₁, *C*₁₂, *C*₁₃, *C*₃₃, *C*₄₄ and *C*₆₆) and elastic moduli (*B*, *G*, *Y*, *B/G* and ν) of tetragonal crystal system Ta₅GeB₂ are calculated and listed in the Table 2. The newly synthesized T₂ phase satisfies the mechanical stability conditions for tetragonal crystal [43]: *C*₁₁ > 0, *C*₃₃ > 0, *C*₄₄ > 0, *C*₆₆ > 0, *C*₁₁ - *C*₁₂ > 0, *C*₁₁ + *C*₃₃ - 2 *C*₁₃ > 0, 2(*C*₁₁ + *C*₁₂) + *C*₃₃ + 4 *C*₁₃ > 0. The elastic constants *C*₁₁ and *C*₃₃ describe the linear compression resistance along the directions *a* and *c*, respectively. As can be seen that the calculated elastic constants *C*₁₁ and *C*₃₃ are very large compared to other elastic constants, indicating that the Ta₅GeB₂ system is very incompressible under uniaxial stress along the directions *a* and *c*. The elastic constant *C*₃₃ is much larger than *C*₁₁, meaning that the incompressibility along the direction *c* is much higher. Indeed, the bonds collateral with the *c*-axis show a dominating effect on *C*₃₃ making it much larger than *C*₁₁. Because of *C*₁₁+*C*₁₂ > *C*₃₃, the bonding in the (001) plane is more rigid elastically than that along the *c*-axis as well as the elastic tensile modulus is higher on the (001) plane than that along the *c*-axis. As *C*₄₄ is an important parameter to describe the indentation hardness [44], it is expected that the hardness of Ta₅GeB₂ should be similar to that of Mo₅SiB₂.

Table 2

Single crystal elastic constants *C*_{ij}, polycrystalline bulk modulus *B*, shear modulus *G*, and Young's modulus *Y*, in GPa, Pugh's ratio *G/B*, and Poisson ratio ν of Ta₅GeB₂ in comparison with other T₂ phase.

Crystals	<i>C</i> ₁₁	<i>C</i> ₁₂	<i>C</i> ₁₃	<i>C</i> ₃₃	<i>C</i> ₄₄	<i>C</i> ₆₆	<i>B</i>	<i>G</i>	<i>Y</i>	<i>B/G</i>	ν	References
Ta ₅ GeB ₂	340	124	137	391	169	137	230	152	374	1.51	0.23	[This]
Mo ₅ SiB ₂	483	154	188	419	179	127						[36]
	479	174	203	390	163	138						[35]
	480	166	197	415	174	143	277	151	383	1.83	0.27	[45]
Ta ₅ GeC ₄	460	162	197	384	166	148	268	143	365	1.87	0.27	[49]

In the present calculations, *C*₄₄ > *C*₆₆, which insures that the new T₂ superconductor Ta₅GeB₂ is Cr₅B₃-prototype phase and in which the [100](010) shear is easier than the [100](001) shear. The shear anisotropy factor *A*, $[= 2C_{66}/(C_{11} -$

$C_{12})$ is found to be 1.27. This indicates that for the (001) plane of Ta_5GeB_2 the shear elastic properties are strongly dependent on the shear directions.

Cauchy pressure, Pugh's ratio (B/G) and Poisson ratio (ν) are regarded as a measure to predict the failure mode, i.e., ductile versus brittle nature, of materials. Materials which easily change their volumes are brittle and materials which can be easily distorted are ductile. The Cauchy pressure ($C_{12} - C_{44}$) is considered to serve as an indication of ductility/brittleness of materials. The material is likely to be ductile (brittle) when the pressure is positive (negative). A different index of the ductility/brittleness is the Pugh ratio (B/G). The high or low ratio is linked to the ductile or brittle nature. To take apart the ductile materials from brittle ones, the critical value is found to be 1.75. Frantsevich et al. [46] also indicated the separation of the ductility from brittleness of materials on the basis of Poisson ratio. Frantsevich rule suggests $\nu \sim 0.26$ as the border line which separates the brittle from ductile materials. If the Poisson ratio is greater than 0.26 then the material will be ductile otherwise the material will be brittle. The Cauchy pressure ($C_{12} - C_{44}$) of Ta_5GeB_2 is negative, its Pugh ratio B/G is 1.51 which is less than 1.75 and its Poisson ratio ν is 0.23 which is less than 0.26. So, the compound Ta_5GeB_2 should be brittle in nature.

Bulk modulus B assesses the resistance to fracture and shear modulus G estimates the resistance to plastic deformation of polycrystalline materials. The bulk modulus bears a little connection with hardness, as is well known from dislocation theory [47]. On the other hand, a better correlation is observed between hardness and shear modulus. Indeed, the hardness is more sensitive to the shear modulus than the bulk modulus. Therefore, the hardness of Ta_5GeB_2 and Mo_5SiB_2 are expected to be similar.

The Young's modulus Y evaluates the resistance against longitudinal tensions. In addition, the Young's modulus has influence on the thermal shock resistance of a material, as the critical thermal shock coefficient R is inversely proportional to the Young's modulus Y [48]. The larger the R value, the better the thermal shock resistance. The thermal shock resistance is an essential indicator for thermal barrier coating (TBC) materials selection. The small Y value indicates that Ta_5GeB_2 is more resistant to thermal shock than Mo_5SiB_2 . All of its elastic properties are also compared with a MAX phase compound Ta_5GeC_4 [49]. In this system the only difference is B against C. Surprisingly, excepting C_{11} , all of its elastic properties match quite well with the results obtained for the new T_2 phase superconductor, Ta_5GeB_2 .

3.3 Debye temperature

Debye temperature θ_D is associated with various important properties of materials. In fact, a higher Debye temperature implies a higher phonon thermal conductivity. The excitation due to vibration at low temperatures arises solely from acoustic vibrations. In order to estimate the magnitude of Debye temperature from the mean sound velocity, we used the following equation [50]:

$$\theta_D = h/k_B [(3n/4\pi)N_A\rho/M]^{1/3}v_m$$

where M is the molecular mass, n is the number of atoms per formula unit, and ρ is the mass density; h is the Plank's constant, k_B is the Boltzmann constant, and N_A is the Avogadro's number. For polycrystalline material the average sound velocity is expressed as [50]:

$$v_m = [1/3(1/v_l^3 + 2/v_t^3)]^{-1/3}$$

where v_l and v_t represent the longitudinal and transverse sound velocities in an isotropic material. These can be determined in terms of bulk modulus B and shear modulus G :

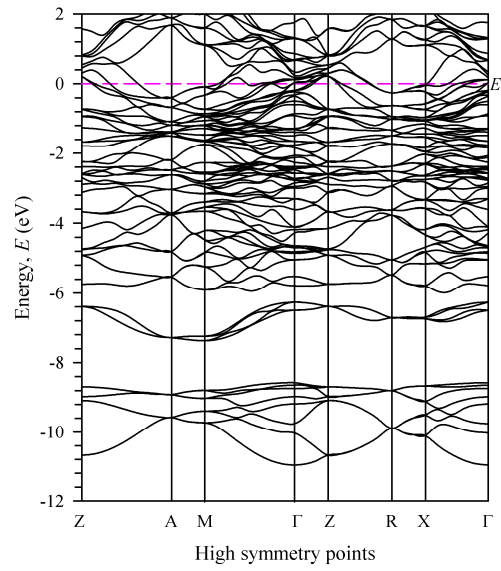
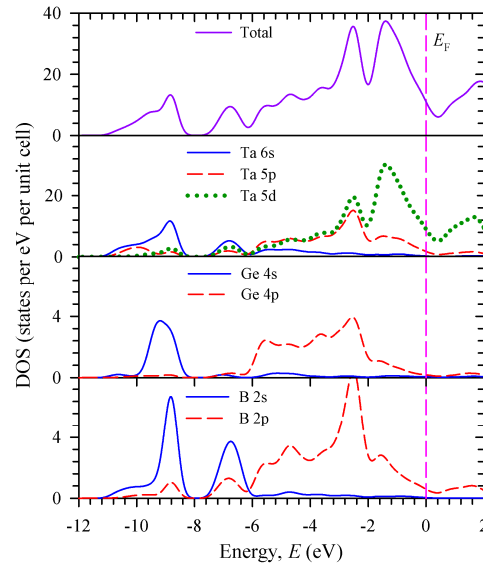
$$v_l = [(3B + 4G)/3\rho]^{1/2} \text{ and } v_t = [G/\rho]^{1/2}.$$

The calculated value of Debye temperature is listed in Table 3 along with measured value as well as with the values for other T_2 phase. The calculated result is deviated by 7.76% from the experimental value. This deviation is expected because the calculation is done on perfect crystal while the measured values are dependent on the purity of the sample, in which impurities, defects, and grain boundaries may be present. The theoretical result predicts that the new compound has a relatively low θ_D , indicating that it possesses a rather flexible lattice and hence low thermal conductivity.

Table 3

Calculated mass density (ρ in gm/cm³), longitudinal, transverse and sound velocities (v_b , v_t , and v_m in km/s) and Debye temperature (θ_D in K) of Ta₅GeB₂ in comparison with Mo₅SiB₂.

T ₂ phase	ρ	v_l	v_t	v_m	θ_D	References
Ta ₅ GeB ₂	14.7	3.216	5.425	3.561	375	Calc. [This]
					348	Expt. [1]
Mo ₅ SiB ₂					592	Calc. [45]
					515	Expt. [38]

**Figure 2** Electronic band structure of T₂ phase Ta₅GeB₂.**Figure 3** Total and partial DOS of Ta₅GeB₂. The Fermi level E_F is set at 0 eV.

3.4 Band structure and DOS

The electronic properties of new ternary compound Ta_5GeB_2 is investigated by calculating the band structure and total as well as partial DOSs. The calculated band structure at equilibrium lattice constants is drawn along high symmetric directions in the first Brillouin zone [Fig. 2]. The Fermi level of new T_2 superconductor lies below the valence bands maximum near the Γ point. The new T_2 phase is observed to be metallic in nature since there is a overlapping of valence bands with conduction bands.

The nature of bonding of solids may be suitably predicted through partial DOS analysis. To describe the electronic structure and bonding nature, the total and partial DOSs are shown in Fig. 2b. The large value of DOS at E_F assures once again the metallic nature of new T_2 superconductor Ta_5GeB_2 . The Fermi level lies to the left of a deep valley named pseudogap E_p , which indicates the stability of the structure. Electrons situated at levels above E_p become delocalized and the material becomes metalized. Mainly Ta 5d states contribute to the DOS at the Fermi level with small contribution from p states of Ta and B. The calculated DOS at the Fermi level is found to be 11.4 states/cell/eV. This large value indicates the high metallic conductivity of the new compound.

The valence bands lying in the lowest energy range of -11.1 to -8.2 eV originates mainly from Ta 6s states with admixture from Ge 4s and B 2s states. These valence bands are seen to be separated by a narrow forbidden gap of ~0.6 eV from the higher valence bands situated in the energy range from -7.6 eV to E_F . The wide higher valence band possesses several distinct peaks. It is seen that the left peak structure between -7.6 and -6.2 eV is formed almost entirely by Ta 6s and B 2s states. The next structures in the total DOS situated between -6.2 and -3.3 eV are mainly due to Ta 5p and 5d states as well as Ge 4p and B 2p states. The second highest peak, between -3.3 and -2.0 eV consists of Ta 5d and 5p states. The highest peak between -2.0 eV and E_F is formed from the strong hybridization of p and d states of Ta with p states of Ge and B. It is obvious that within the range from -7.6 eV to E_F , there occurs a covalent interaction between the constituting atoms. This is due to the reason that states are really degenerate with respect to angular momentum and lattice site. Further, some degree of ionic character is expected simply for the difference in the value of electronegativity among the comprising elements.

3.5 Mulliken atomic populations

The Mulliken population analysis can facilitate to assign the electrons in several fractional methods among the various parts of bonds and overlap population has correlations with covalency or ionicity of bonding and bond strength. Population analysis in CASTEP is carried out using a projection of the plane wave states onto a localized basis by means of a technique developed by Sanchez-Portal et al. [51]. Population analysis of the resulting projected states is then accomplished by using the Mulliken formalism [52]. This method is widely used in the analysis of electronic structure calculations performed with Linear Combination of Atomic Orbitals (LCAO) basis sets. The most essential quantities in relation to atomic bond population calculations are the effective charge and the bond order values between pairs of bonding atoms using minimal basis within the Mulliken scheme [52,53] as follows:

$$Q_{\alpha}^* = \sum_{i,\alpha} \sum_{n \text{ occ}} \sum_{j,\beta} C_{i\alpha}^{*n} C_{j\beta}^n S_{i\alpha,j\beta}$$

$$\rho_{\alpha\beta} = \sum_{n \text{ occ}} \sum_{i,j} C_{i\alpha}^{*n} C_{j\beta}^n S_{i\alpha,j\beta}$$

where i, j stand for the orbital quantum numbers and n is the band index, $C_{i\alpha}^{*n}$ as well as $C_{j\beta}^n$ are the eigenvector coefficients of the wave function and $S_{i\alpha,j\beta}$ is the overlap matrix between atoms α and β .

The effective valence charge and Mulliken atomic population constantly assist to realize the bonding nature in solids. The difference between the formal ionic charge and Mulliken charge on the anion species in the crystal estimates the effective valence and verifies the ascendancy of covalent and ionic bonding. An ideal ionic bond is observed when the effective valence has zero value. On the contrary, an increasing level of covalency is seen if the effective valence carries a value greater than zero. The effective valence listed in the Table 4 would be a sign of the prominent covalency in bonding within the new ternary T_2 phase Ta_5GeB_2 . The calculated bond overlap populations for the new ternary T_2 phase superconductor listed in Table 5. The overlap population of nearly zero value signifies that the interaction between the electronic populations of the two atoms is insignificant. A bond associated with a smallest Mulliken population is extremely weak and which plays insignificant role in the materials hardness. A low overlap population is a sign of a high degree of ionicity, whereas a high value implies a high degree of covalency in the chemical bond. The bonding and anti-

bonding states arise due to positive and negative bond overlap populations, respectively. It is seen that the B–B bonds are more covalent than the Ta–Ta bonds.

Table 4 Population analysis of Ta₂GeB₂.

Species	Mulliken Atomic populations					Effective valence Charge (e)
	s	P	d	Total	Charge(e)	
B	1.18	2.53	0.00	3.72	– 0.72	--
Ge	– 0.75	3.00	0.00	2.25	1.75	2.25
Ta 1	0.63	0.38	3.90	4.91	0.09	4.91
Ta 2	0.64	0.60	3.86	5.10	– 0.10	5.10

3.6 Theoretical Vickers hardness

Hardness is defined as the ability of a material to resist plastic deformation. The resistant force acted on per unit area takes part in estimating the hardness of a material. To evaluate the hardness of non-metallic materials a formula is developed with Mulliken population in first-principles method [54]. This method is not applicable for compounds with partial metallic bonding like T₂ phases because metallic bonding is delocalized and has no direct relation with hardness [55]. To calculate the hardness of metallic crystals, a correction for metallic bonding in the formula should be taken into account. Gou et al. [56] proposed a formula including such correction for the bond hardness of a crystal having partial metallic bonding as follows:

$$H_v^\mu = 740(P^\mu - P^{\mu'}) (v_b^\mu)^{-5/3}$$

where P^μ represents the Mulliken overlap population of the μ -type bond, $P^{\mu'}$ is symbolized for the metallic population and is calculated using the unit cell volume V and the number of free electrons in a cell $n_{free} = \int_{E_F}^{E_P} N(E)dE$ as $P^{\mu'} = n_{free}/V$, and v_b^μ stands for the volume of a bond of μ -type, which is evaluated from the bond length d^μ of type μ and the number of bonds N_b^ν of type ν per unit volume by $v_b^\mu = (d^\mu)^3 / \sum_\nu [(d^\mu)^3 N_b^\nu]$. The hardness for the complex multiband crystals can be calculated as a geometric average of all bond harnesses as follows [57,58]:

$$H_V = [\prod (H_v^\mu)^{n^\mu}]^{1/\sum n^\mu}$$

where n^μ is the number of bond of type μ composing the actual multiband crystal. The obtained value of the Vickers hardness for the newly synthesized compound is listed in Table 5. The hardness value of 14.6 GPa for Ta₅GeB₂ is slightly less than the room temperature Vickers hardness of around 18 GPa for Mo₅SiB₂ [45]. It is, still, essential to note that the calculated Vickers hardness is only 15.2% that of diamond (96 GPa), which stays behind the hardest material known to date.

Table 5

Calculated bond and Vickers hardness H_v^μ , H_v (in GPa) of Ta₅GeB₂ along with bond number n^μ , bond length d^μ (Å), bond volume v_b^μ (Å³) and bond and metallic populations P^μ , $P^{\mu'}$.

Bond	n^μ	d^μ	P^μ	$P^{\mu'}$	v_b^μ	H_v^μ	H_v
B–B	4	2.10100	0.40	0.1084	2.2027	57.87	14.6
B–Ta	32	2.44347	0.34	0.1084	3.4649	21.60	
	16	2.53161	0.44	0.1084	3.8536	25.91	
	16	2.53545	0.26	0.1084	3.8711	11.75	
Ta–Ta	32	2.86824	0.30	0.1084	5.6043	8.02	
	8	2.97855	0.35	0.1084	6.2761	8.37	

4. Conclusion

In this paper, first-principles investigations have been carried out on the structural parameters, single crystal as well as polycrystalline elastic properties, Debye temperature, band structure, DOS, Mulliken atomic population and theoretical Vickers hardness of newly synthesized Ta₅GeB₂ for the first time. The calculated lattice parameters show good agreement with the measured values. The mechanical properties are estimated from the calculated elastic constants. Born criteria for tetragonal crystal are satisfied, suggesting that the new compound Ta₅GeB₂ is mechanically stable. Cauchy pressure, Pugh's ratio and Poisson ratio predict that Ta₅GeB₂ should be characterized as brittle material. The small value of Y indicates that Ta₅GeB₂ should have good thermal shock resistance. The relatively low Debye temperature of 375 K should be a sign of flexible lattice as well as low thermal conductivity. The bonding nature of Ta₅GeB₂ may be explained as a mixture of metallic, covalent and ionic. In Ta₅GeB₂, the B–B bonds are more covalent than the Ta–Ta bonds. The calculated hardness value of 14.6 GPa for Ta₅GeB₂ is 15.2% of (96 GPa) for diamond, which is the hardest known material.

References

- [1] L. E. Corrêa, M. S. da Luz, B. S. de Lima, O. V. Cigarroa, A. A. A. P. da Silva, G. C. Coelho, Z. Fisk, A. J. S. Machado, J. Alloys Comp. **660**, 44 (2016).
- [2] W. B. Pearson, The crystal Chemistry and Physics of Metals and Alloys (Wiley-Interscience, New-York, 1972).
- [3] B. Aronsson, Acta Chem. Scand. **12**, 31 (1958).
- [4] B. Aronsson and G. Lundgren, Acta Chem. Scand. **13**, 433 (1959).
- [5] I. Schewe-Miller, P. Böttcher, and H. G. von Schnering, Z. Kristallogr. **188**, 287 (1989).
- [6] I. Schewe-Miller and P. Böttcher, Z. Kristallogr. **196**, 137 (1991).
- [7] R. Kubiak, Z. Anorg. Allg. Chem. **431**, 261 (1977).
- [8] R. Wang, B. C. Giessen and N. J. Grant, Z. Kristallogr. **129**, 244 (1969).
- [9] J. V. Hutcherson, R. L. Guay and J. S. Herold, J. Less-Common Met. **11**, 296 (1969).
- [10] H. Ullmaier, R. H. Kernohan, E. Cruceanu and E. Hering, J. Low Temp. Phys. **5**, 71 (1971).
- [11] A. Juodakis and C. R. Kannewurf, J. Appl. Phys. **39**, 3003 (1968).
- [12] E. Cruceanu and St. Slădaru, J. Mater. Sci. **4**, 410 (1969).
- [13] S. Bhan and K. Schubert, J. Less-Common Met. **20**, 229 (1970).
- [14] W. H. Haemmerle, W. A. Reed, A. Juodakis and C. R. Kannewurf, J. Appl. Phys. **44**, 1356 (1973).
- [15] C. A. Nunes, R. Sakidja, Z. Dong, and J. H. Perepko, Intermetallics **8**, 327 (2000).
- [16] M. K. Meyer and M. Akinc, J. Am. Ceram. Soc. **79**, 938 (1996).
- [17] M. K. Meyer and M. Akinc, J. Am. Ceram. Soc. **79**, 2763 (1996).
- [18] M. K. Meyer, A. J. Thom and M. Akinc, Intermetallics **7**, 153 (1999).
- [19] J. J. Kruzic, J. H. Schneibel, and R. O. Ritchie, Metall. Mater. Trans. A **36A**, 2393 (2005).
- [20] H. Choe, D. Chen, J. H. Schneibel, R.O. Ritchie, Intermetallics **9**, 319 (2001).

- [21] M. K. Meyer, M. J. Kramer and M. Akinc, *Adv. Mater.* **8**, 85 (1996).
- [22] M. K. Meyer, M. J. Kramer and M. Akinc, *Intermetallics* **4**, 273 (1996).
- [23] T. G. Nieh, J. G. Wang and C. T. Liu, *Intermetallics* **9**, 73 (2001).
- [24] J. H. Schneibel, C. T. Liu, D. S. Easton and C. A. Carmichael, *Mater. Sci. Eng. A* **261**, 78 (1999).
- [25] F. Chu, D. J. Thoma, K. J. McClellan, P. Peralta, E. Fodran, *MRS Proceedings* **552** (1998) KK6.7.1
- [26] P. Hohenberg and W. Kohn, *Phys. Rev.* **136**, B864 (1964).
- [27] W. Kohn and L. J. Sham, *Phys. Rev.* **140**, A1133 (1965).
- [28] S. J. Clark, M. D. Segall, C. J. Pickard, P. J. Hasnip, M. I. J. Probert, K. Refson, M. C. Payne, *Z. Kristallogr.* **220**, 567 (2005).
- [29] J. P. Perdew, K. Burke and, M. Ernzerhof, *Phys. Rev. Lett.* **77**, 3865 (1996).
- [30] Vanderbilt, *Phys. Rev. B* **41**, 7892 (1990).
- [31] H. J. Monkhorst and J. D. Pack, *Phys. Rev. B* **13**, 5188 (1976).
- [32] T. H. Fischer and J. Almlof, *J. Phys. Chem.* **96**, 9768 (1992).
- [33] R. Sakidja, J. H. Perepezko, S. Kim and N. Sekido, *Acta Mater.* **56**, 5223 (2008).
- [34] J. -M. Joubert, C. Colinet, G. Rodrigues, P. A. Suzuki, C. A. Nunes, G. C. Coelho and J. -C. Tedenac, *J. Solid State Chem.* **190**, 111 (2012).
- [35] S. Aryal, M. C. Gao, L. Ouyang, P. Rulis, W. Y. Ching, *Intermetallics* **38**, 116 (2013).
- [36] R. D. Fielda, D. J. Thomaa, J. C. Cooleya, F. Chua, C. L. Fub, M. H. Yoob, W. L. Hultsa and C. M. Cadya, *Intermetallics* **9**, 863 (2001).
- [35] S. Aryal, M. C. Gao, L. Ouyang, P. Rulis, W. Y. Ching, *Intermetallics* **38**, 116 (2013).
- [36] R. D. Fielda, D. J. Thomaa, J. C. Cooleya, F. Chua, C. L. Fub, M. H. Yoob, W. L. Hultsa and C. M. Cadya, *Intermetallics* **9**, 863 (2001).
- [37] R. J. Rawn, J. H. Schneibel, C. M. Hoffmann and C. R. Hubbard, *Intermetallics* **9**, 209 (2001).
- [38] A. J. S. Machado, A. M. S. Costa, C. A. Nunes, C. A. M. dos Santos, T. Grant and Z. Fisk, *Solid State Commun.* **151**, 1455 (2011).
- [39] F. D. Mumaghan, *Finite Deformation of an Elastic Solid* (Wiley, New York, 1951).
- [40] W. Voigt, *Lehrbuch der Kristallphysik* (Taubner, Leipzig, 1928).
- [41] A. Reuss, *Z. Angew. Math. Mech.* **9**, 49 (1929).
- [42] R. Hill, *Proc. Phys. Soc. A* **65**, 349 (1952).
- [43] M. Born, K. Huang and M. Lax, *Am. J. Phys.* **23**, 474 (1995).
- [44] H. Koc, H. Ozisik, E. Deligöz, A. M. Mamedov and E. Ozbay, *J. Mol. Model.* **20**, 2180 (2014).
- [45] K. Ihara, K. Ito, K. Tanaka and M. Yamaguchi, *Mater. Sci. Engin. A* **329–331**, 222 (2002).
- [46] I. N. Frantsevich, F. F. Voronov, and S.A. Bokuta, *Elastic constants and elastic moduli of metals and insulators handbook* (Naukova Dumka, Kiev, 1983), pp. 60–180.
- [47] J. H. Westbrook and H. Conrad (eds), *Conference Proceedings on The Science of Hardness Testing and Its Research Applications*, (ASM, Metals Park, Ohio, 1973).
- [48] X. Wang, H. Xiang, X. Sum, J. Liu, F. Hou and Y. Zhou, *J. Mater. Sci. Tech.* **31**, 369 (2015).
- [49] S. Aryal, R. Sakidja, M. W. Barsoum and W. Y. Ching, *Phys. Status Solidi B*, 251, 1480 (2014).
- [50] O. L. Anderson, *J. Phys. Chem. Solids* **24**, 909 (1963).
- [51] D. Sanchez-Portal, E. Artacho, and J. M. Soler, *Solid State Commun.*, **95**, 685 (1995).
- [52] R. S. Mulliken, *J. Chem. Phys.* **23**, 1833 (1955).
- [53] W. Y. Ching and P. Rulis, *Electronic Structure Methods for Complex Materials -The orthogonalized Linear combination of atomic orbitals*, (Oxford Univ. Press, 2012).
- [54] F. M. Gao, *Phys. Rev. B* **73**, 132104 (2006).
- [55] J. H. Westbrook and H. Conrad, *The Science of Hardness Testing and Its Research Applications* (ASM, Ohio, 1973).
- [56] H. Gou, L. Hou, J. Zhang and F. Gao, *Appl. Phys. Lett.* **92**, 241901(2008).
- [57] A. Szymański and J. M. Szymański, *Hardness Estimation of Minerals Rocks and Ceramic Materials*, 6th edition, (Elsevier, Amsterdam, 1989).
- [58] V. M. Glazov and V. N. Vigdorovid, *Hardness of Metals* (Izd. Metellurgiya, Moskva, 1989).